34. MATHEMATICAL TREATMENT OF GEOCHEMICAL DATA, DEEP SEA DRILLING PROJECT SITES 415 AND 416

P. Debrabant, J. Foulon, and H. Maillot, U.E.R. des Sciences de la Terre,
Université des Sciences et Techniques de Lille, 59650 Villeneuve d'Ascq, France

ABSTRACT

We collected geochemical data from 94 samples from DSDP Leg 50. With the help of multivariate analyses (correlations, factor analysis in principal components) we stress the essential characteristics of the geochemical environment of Sites 415 and 416, and show analogies with the other DSDP holes of the eastern Atlantic margin. Sediments from Site 416 are dominantly ferro-potassic, a detrital deposit containing primary Cretaceous minerals. The Site 415 sediments are more ferro-magnesian; there is a correspondence with prevalent smectites marked by the same trace elements (Ti Cr V) at Sites 398 to 402. Contents of the major elements are similar, showing continuity of the origin of the detrital supply.

The environment became more open between Albian and Aptian time. Sediments of the two sites show numerous similarities from that level upward and a geochemical break is indicated somewhere between Paleocene and Miocene.

MATHEMATICAL TREATMENT OF THE GEOCHEMICAL DATA

Introduction

The predominance of detrital material in the sediments analyzed makes a precise geochemical study and establishment of a detailed geochemical zonation difficult. Our analyses were made from the same samples as those analyzed by Chamley (this volume) and we shall refer to the mineralogical results he obtained.

The results of the geochemical analyses are shown in Tables 1 and 3.

General Considerations on the Geochemistry of Leg 50

Site 415 (Tables 1 and 2)

The very sparse sampling does not permit great precision in the study of samples from this site. Most of the samples fall into a relatively dense cluster in the Al_2O_3, Fe_2O_3, MgO diagram (Figure 1); a few more-magnesian or more-ferruginous samples are isolated. The data points of lithologic Units IV, V, VI are more markedly dispersed. The study shows that the corresponding samples from Units I, II, and III are geochemically different and show a marked discontinuity between Paleocene and Miocene sediments.

The Miocene and overlying sediments, as seen from the Sr/CaO ratio, are usually calcareous (50 to 70% $CaCO_3$) accompanied by high strontium concentrations. The calcareous samples of the lower series do not have high strontium concentrations. This is a general tendency in the sediment of the eastern Atlantic margin sites (Chamley et al., 1979; Debrabant et al., 1979).

In addition, certain transition elements (Mn, Cr, V) occur in lower concentrations or in different associations within the Paleocene and Miocene sediments. In Miocene and overlying sediments, the occurrence of manganese does not seem to be related to that of carbonates. This can be caused either by a difference in the degree of carbonate diagenesis or to a distinct change in the redox conditions of the depositional environment (a more reducing environment in the lower series).

Furthermore, the MgO/K_2O, Al_2O_3/K_2O, and Fe_2O_3/K_2O ratios decrease toward the top of the hole owing to an increase in the supply of potassic clay and a relative decrease in smectites. (The illite increases more rapidly than the chlorite, which masks the ferromagnesian composition of that clay.) Lastly, the transition from Cretaceous to Tertiary sediments is accompanied by a slight increase of phosphate occurring in the Cenomanian (only traces in Sample 415A-8-1, 110 cm), reaching 0.57 per cent P_2O_5 in the Paleocene and diminishing in the Miocene (0.23% in Sample 415-5-3, 40 cm).

A similar phenomenon occurs in sediments of approximately the same age from Site 416, and P_2O_5 is also traceable in the Cenomanian and Paleocene at Site 398 (Debrabant et al., unpublished manuscript). This might have resulted from a pre-existing deep current or the initiation of a new current, as is suggested by the presence of siliceous organisms in the sediments of both sites.

Site 416 (Tables 3, 4)

All samples analyzed contained very low concentrations of carbonate. The greatest amounts of 63 per cent and 73 per cent occur in upper Tithonian and Miocene

TABLE 1
Geochemical Analyses, Site 415[a]

Sample (interval in cm)	SiO_2	Al_2O_3	CaO	MgO	Na_2O (%)	K_2O	TiO_2	P_2O_5	Fe_2O_3	Mn	Zn	Li	Ni	Cr (ppm)	Sr	Co	Cu	Pb	V
415A–1–5, 100	18.00	6.26	34.90	1.78	1.55	1.54	0.31	n.d.	2.52	260	74	37	35	39	1150	16	64	37	79
415A–1–6, 14	24.30	7.85	29.19	2.13	1.67	1.91	0.40	n.d.	3.33	260	76	45	31	49	900	14	17	18	105
415B–2–1, 44	12.15	3.84	40.60	1.33	1.11	1.14	0.20	n.d.	1.64	290	33	23	23	37	1350	8	12	24	47
415B–2–1, 91	20.15	6.31	33.08	2.04	1.26	1.63	0.32	n.d.	2.50	210	79	42	36	43	1200	15	13	21	89
415B–3–1, 62	16.95	4.72	36.19	1.73	1.13	1.33	0.24	n.d.	2.06	200	50	34	35	41	1350	15	18	21	84
415B–3–3, 62	24.55	6.32	30.45	1.78	1.18	1.55	0.33	n.d.	2.50	150	64	37	35	45	1250	13	16	6	105
415B–4–1, 6	17.50	4.96	35.77	1.90	1.01	1.45	0.23	n.d.	2.13	200	53	31	35	44	1350	13	18	32	47
415B–5–3, 40	23.50	4.25	32.90	1.58	0.98	1.16	0.22	0.23	1.33	250	69	34	34	39	1050	13	22	25	37
415B–5–5, 33	30.35	6.61	25.94	2.48	1.20	1.69	0.36	n.d.	3.14	200	79	53	35	58	850	9	21	22	47
415B–5–6, 27	23.00	4.13	33.60	1.60	1.11	1.10	0.21	n.d.	1.69	150	55	36	25	45	1200	9	16	24	58
415A–5, CC, 1	63.20	13.60	0.88	2.82	2.24	1.44	0.56	0.23	4.64	150	150	36	48	200	350	17	250	14	175
415A–6–1, 112	32.90	3.48	27.86	1.60	1.42	0.56	0.13	0.57	1.39	650	67	25	31	95	750	2	33	13	63
415A–7–1, 24	57.70	15.35	1.86	3.17	1.95	2.14	0.67	0.43	6.07	300	130	42	58	150	350	18	61	16	180
415A–8–1, 110	44.35	13.60	9.66	3.92	1.60	1.20	0.75	n.d.	5.64	600	69	30	42	120	400	13	4	16	160
415A–9–1, 95	31.90	10.27	22.05	1.80	1.15	0.66	0.70	n.d.	4.50	380	66	20	27	83	550	16	1	30	120
415A–10–1, 78	45.50	13.93	8.51	3.87	1.16	2.35	0.70	n.d.	6.26	530	89	46	35	110	350	18	16	89	130
415A–11–1, 12	38.20	12.81	15.86	2.30	1.21	0.90	0.79	n.d.	6.00	400	84	40	25	90	450	15	1	13	170
415A–12–1, 113	42.35	12.40	13.86	1.86	1.40	0.96	0.83	n.d.	5.36	300	89	34	31	100	600	15	1	12	140
415A–13–1, 125	21.35	5.37	34.82	1.61	0.59	0.65	0.33	n.d.	6.14	650	47	20	18	47	650	16	1	25	89

[a]Organic carbon not determined.

TABLE 2
Geochemical Ratios, Site 415

Sample (interval in cm)	$\frac{SiO_2}{Al_2O_3}$	$\frac{Al_2O_3}{Fe_2O_3}$	$\frac{MgO}{K_2O}$	$\frac{Al_2O_3}{K_2O}$	$\frac{Na_2O}{K_2O}$	$\frac{Fe_2O_3}{K_2O}$	$\frac{Fe_2O_3}{MgO}$	$\frac{Sr\ 10^3}{CaO}$
415–1–5, 100	2.9	2.5	1.2	4.1	1.01	1.6	1.4	3.3
415–1–6, 140	3.1	2.4	1.1	4.1	0.87	1.7	1.6	3.1
415B–2–1, 44	3.2	2.3	1.2	3.4	1.00	1.4	1.2	3.3
415B–2–1, 91	3.2	2.5	1.3	3.9	0.77	1.6	1.2	3.6
415B–3–1, 62	3.6	2.3	1.3	3.6	0.85	1.6	1.2	3.7
415B–3–3, 62	3.9	2.5	1.2	4.1	0.76	1.6	1.4	4.1
415B–4–1, 6	3.5	2.3	1.3	3.4	0.70	1.5	1.1	3.8
415B–5–3, 4	5.5	3.2	1.4	3.7	0.84	1.2	0.8	3.2
415B–5–5, 33	4.6	2.1	1.5	3.9	0.71	1.9	1.3	3.3
415B–5–6, 27	5.6	2.4	1.5	3.8	1.01	1.5	1.1	3.6
415A–5, CC, 1	4.7	2.9	2.0	9.4	1.56	3.1	2.1	39.8
415A–6–1, 112	9.5	2.5	2.9	6.2	2.54	2.5	0.9	2.7
415A–7–1, 24	3.8	2.5	1.5	7.2	0.91	2.8	1.9	18.8
415A–8–1, 110	3.3	2.4	3.3	11.3	1.33	4.7	1.4	4.4
415A–9–1, 95	3.1	2.3	2.7	15.6	1.74	6.8	2.5	2.5
415A–10–1, 78	3.3	2.2	1.7	5.9	0.49	2.7	1.6	4.1
415A–11–1, 12	3.0	2.1	2.6	14.2	1.34	6.7	2.6	2.8
415A–12–1, 113	3.4	2.3	1.9	12.9	1.46	5.6	2.9	4.3
415A–13–1, 125	4.0	0.9	2.5	8.3	0.91	9.5	3.8	2.8

samples, respectively. Conversely, many samples contain less than 5 per cent $CaCO_3$. Complete dissolution could have occurred at two levels (Hauterivian and Aptian), but the samples do not have any resulting accumulations of metals.

The silicate phase, consequently, largely predominates in the cores, and high titanium concentrations confirm the detrital origin of most of the sediments. A few Tithonian to Valanginian samples and some Aptian to Barremian are particularly siliceous. Their high SiO_2/Al_2O_3 ratios imply the presence of free silica.

Most of the samples from Units VI and VII are grouped in a very restricted area on the Al_2O_3, Fe_2O_3, MgO diagram (Deer et al., 1963). A few particularly ferriferous or magnesian samples appear as isolated points (Figure 2). On the other hand, most of the Eocene and post-Eocene samples gather outside that zone. This tendency was also noted in the Site 415 samples.

A comparison between the respective domains of Sites 415 and 416 (Figure 2) also shows that the pre-Albian samples clearly group toward the aluminum apex (Site 416), which implies distinct clay sources before and after that epoch. Kaolinite is important in this regard.

Samples from Site 416 do not contain significantly high concentrations of magnesium, which confirms the paucity of dolomite. Two slightly phosphatic levels occur in upper Eocene and Miocene sediments.

No zone is significantly enriched in iron or in transition metals. Lithium and vanadium are highly concentrated, however, compared to the sediments of Legs 47B and 48. Apparently this is related to a high illite content as it correlates with high values for K_2O. Finally, the organic carbon is traceable in quantities larger than 1 per cent only in the Hauterivian sediments.

Mathematical Treatment of the Geochemical Data

We shall not compare the data from the multivariate studies between sites because only the post-Aptian sequence is common to both Sites 415 and 416. This comprises only eight samples, whereas we treat 75 samples in the mathematical study.

Mean Chemical Compositions (Table 5)

The standard deviations are naturally high because of the heterogeneity of the materials analyzed. However, sediments from Site 416 tend to have more silicate and less carbonate. A study of the probable variation range, however, shows that the chemical-element concentrations, except for potassium and lithium, all overlap. The particular relationship between those two elements is

TABLE 3
Geochemical Analyses, Site 416

Sample (interval in cm)	SiO_2	Al_2O_3	CaO	MgO	Na_2O	K_2O	TiO_2	P_2O_5	Fe_2O_3	C_{org}[a]	Mn	Zn	Li	Ni	Cr	Sr	Co	Cu	Pb	V
	(%)										(ppm)									
416–1–1, 33	26.60	8.09	27.65	1.94	1.67	1.81	0.44	n.d.	3.50	–	370	77	41	29	54	900	15	34	110	105
416–1–1, 44	13.10	3.89	40.60	1.36	0.89	1.23	0.14	n.d.	1.72	0.15	280	55	24	27	33	1380	14	15	320	32
416–1–1, 99	38.25	7.49	17.36	4.71	1.30	2.45	0.31	0.23	3.70	0.14	400	110	52	28	76	450	9	28	22	63
416–1–1, 117	32.75	8.44	21.98	2.82	1.48	2.21	0.29	n.d.	3.80	–	330	73	49	33	64	750	13	15	95	100
416–1–2, 33	27.80	6.09	28.21	2.33	1.16	1.58	0.20	n.d.	2.63	0.18	390	71	47	26	48	1000	9	33	32	42
416–2–1, 31	41.90	9.62	14.52	3.74	1.28	2.73	0.25	n.d.	4.45	0.25	350	83	72	20	77	480	6	16	9	74
416–2–3, 64	40.65	8.44	17.50	2.88	1.36	2.45	0.26	n.d.	3.92	0.28	300	83	57	21	61	600	6	54	12	63
416–3–3, 39	53.65	13.39	4.41	3.60	1.53	3.52	0.66	n.d.	5.22	0.22	320	107	79	31	125	280	13	29	25	120
416–3–3, 47	41.90	9.38	12.60	3.65	1.28	2.85	0.60	0.34	4.43	0.71	340	95	59	45	120	440	15	15	22	110
416–6–3, 3	65.65	14.31	0.21	1.83	1.45	3.60	0.71	n.d.	5.00	0.01	180	67	60	39	114	240	13	45	16	95
416–7–2, 122	56.15	17.09	2.80	2.25	1.28	3.61	0.83	n.d.	5.39	0.32	220	88	94	49	100	320	21	18	27	160
416–9–2, 12	47.30	12.00	11.87	1.93	1.13	2.67	0.73	n.d.	4.93	0.50	400	76	71	39	81	480	14	20	21	120
416–10–1, 61	49.85	18.93	2.69	2.57	1.31	3.88	0.79	n.d.	7.86	0.47	520	87	97	52	110	370	27	26	31	160
416–11–3, 4	49.35	21.77	4.51	2.94	1.25	3.60	0.73	n.d.	6.26	–	290	160	53	92	210	400	26	19	56	140
416–11–3, 9	61.95	16.34	1.78	2.24	1.68	2.90	0.68	n.d.	5.14	–	260	150	37	68	160	280	18	17	50	95
416–12–1, 108	27.75	7.04	27.93	1.76	0.89	1.64	0.30	n.d.	4.10	0.29	810	64	43	34	50	810	14	26	16	47
416–12–1, 147	51.80	19.65	2.20	2.60	1.31	3.95	0.85	n.d.	6.75	0.58	300	100	95	65	110	380	33	32	28	160
416–13–2, 67	41.65	18.15	8.65	2.39	1.06	3.52	0.73	n.d.	6.89	0.34	510	88	110	46	110	500	19	17	22	160
416–14–1, 105	44.05	17.11	8.05	2.69	1.06	3.45	0.83	n.d.	7.15	0.57	510	110	100	56	110	460	22	22	21	168
416–16–1, 25	46.30	19.27	6.30	2.59	1.08	3.84	0.79	n.d.	6.19	0.20	300	85	110	46	100	460	22	13	18	180
416–18–1, 137	35.85	11.47	18.20	2.06	0.93	2.60	0.43	n.d.	5.19	0.35	400	110	72	42	74	600	12	29	18	95
416–19–2, 82	52.80	19.99	0.46	3.15	1.30	4.52	0.81	n.d.	7.22	0.40	320	89	98	60	110	320	31	30	29	160
416–19–2, 101	27.60	8.16	24.85	2.14	0.91	2.02	0.33	n.d.	5.76	0.51	720	66	51	33	53	680	13	30	20	84
416–20–1, 99	47.65	16.90	6.23	2.65	1.26	3.31	0.72	n.d.	6.46	0.32	390	100	87	47	100	360	23	22	15	140
416–21–1, 10	23.55	7.00	29.89	1.86	0.71	1.58	0.28	n.d.	3.77	0.35	730	59	42	30	45	770	14	24	18	89
416–23–2, 16	29.90	10.65	21.70	2.03	0.94	2.23	0.36	n.d.	5.33	2.45	600	98	69	37	67	660	16	35	21	120
416–25–1, 97	51.90	18.93	1.86	2.88	1.40	3.81	0.79	n.d.	7.50	0.32	450	115	90	57	100	320	28	26	28	160
416–25–1, 140	28.10	9.56	26.25	2.07	0.70	1.80	0.41	n.d.	3.57	–	770	130	26	32	95	720	7	31	44	84
416–25–1, 147	48.15	20.86	2.31	3.27	1.21	3.90	0.73	n.d.	8.55	–	420	190	47	170	200	300	33	24	52	120
416–29–3, 23	26.30	7.73	28.00	2.12	0.71	1.60	0.21	n.d.	4.32	0.32	1050	58	44	41	47	730	11	34	15	95
416–30–5, 60	50.35	17.00	5.71	2.91	1.36	3.69	0.73	n.d.	6.72	0.22	420	110	81	44	91	410	16	10	14	130
416–36–1, 16	56.60	13.75	6.30	2.51	1.38	2.74	0.69	n.d.	5.64	0.06	410	72	64	32	75	340	12	6	9	110
416–36–1, 129	42.70	18.88	9.27	2.74	1.00	3.10	0.66	n.d.	6.97	0.19	420	120	49	77	170	460	22	11	68	120
416–36–2, 8	57.10	12.02	8.09	2.25	1.47	2.39	0.60	n.d.	4.79	0.19	480	120	54	35	72	370	18	19	14	95
416–36–3, 28	53.00	20.36	2.55	3.07	1.23	3.20	0.78	n.d.	6.26	0.36	320	140	48	95	190	340	23	18	60	130
416–37–2, 77	54.55	17.69	2.60	2.74	1.18	3.78	0.83	n.d.	6.79	–	320	89	82	53	102	320	26	25	27	150
416–37–3, 10	30.40	6.59	25.24	3.20	0.64	1.57	0.30	n.d.	4.62	0.13	720	58	39	26	26	650	10	31	19	79
416–37–4, 7	48.45	22.26	4.06	2.76	0.93	3.36	0.76	n.d.	7.01	0.11	310	130	61	77	210	370	23	14	63	140
416–38–1, 11	48.05	15.75	10.40	2.49	1.19	3.09	0.63	n.d.	5.26	0.11	370	120	36	41	150	430	15	21	41	95
416–38–1, 44	51.50	13.89	4.34	2.88	1.13	3.76	0.83	n.d.	6.57	0.26	310	85	82	51	100	380	23	46	32	140
416–38–2, 18	33.75	14.93	18.20	2.40	0.78	2.91	0.51	n.d.	5.72	0.19	580	150	36	47	130	550	16	12	63	95
416–40–6, 4	55.65	14.10	3.05	2.89	1.31	3.67	0.79	n.d.	5.86	0.31	330	88	80	51	110	370	32	29	33	150
416–40–6, 17	43.35	18.64	10.46	2.78	0.94	3.16	0.53	n.d.	5.36	0.85	400	150	48	47	160	350	16	17	52	120
416–40–6, 22	52.40	19.94	3.12	3.36	1.25	3.66	0.74	n.d.	7.26	0.14	300	180	39	81	200	370	25	17	74	120
416–42–2, 125	48.95	23.60	3.05	2.86	1.09	3.78	0.68	n.d.	7.55	0.17	310	140	62	87	210	440	26	8	77	140
416–43–1, 46	51.60	17.02	4.66	2.70	1.01	3.67	0.77	n.d.	7.72	0.13	390	97	96	51	84	440	26	15	37	150
416–43–2, 51	51.30	14.99	8.26	2.74	1.33	2.68	0.63	n.d.	5.22	0.11	430	140	29	55	140	350	11	22	59	79
416–43–4, 56	48.85	20.30	4.55	3.19	1.13	3.80	0.73	n.d.	7.62	0.11	320	130	42	74	180	400	20	13	61	130
416–43–4, 80	40.80	15.81	13.05	3.11	1.33	3.06	0.58	n.d.	5.69	0.31	560	190	32	69	160	550	29	47	71	120
416–44–1, 11	50.30	14.75	9.31	2.49	1.35	3.23	0.68	n.d.	5.40	0.03	340	100	28	40	150	390	10	17		79
416–44–2, 1	53.60	21.59	1.22	3.36	1.31	3.98	0.80	n.d.	5.90	0.27	280	170	45	150	220	320	33	31	55	140
416–44–2, 7	54.35	18.41	1.75	3.17	1.26	4.16	0.83	n.d.	6.23	0.01	300	95	86	68	97	370	35	18	36	150
416–44, CC, 12	24.70	10.50	28.35	2.61	0.66	2.28	0.35	n.d.	4.22	0.13	600	130	21	49	100	460	23	14	55	79
416–46–2, 8	58.00	15.69	3.96	2.48	1.50	2.95	0.79	n.d.	4.12	0.13	340	110	69	41	74	350	22	16	23	100
416–46–2, 10	55.05	16.95	3.85	2.71	1.40	3.56	0.75	n.d.	5.32	0.17	330	135	89	47	92	360	27	24	33	140
416–46–4, 100	48.60	17.70	4.83	3.32	1.06	3.67	0.75	n.d.	7.62	0.13	380	110	76	58	91	400	27	25	32	120
416–46–4, 104	60.55	15.16	2.98	2.48	1.58	2.95	0.75	n.d.	3.79	0.16	310	98	63	38	86	310	13	140	27	95
416–46–4, 110	53.85	19.58	2.17	3.35	1.28	4.01	0.79	n.d.	5.57	0.19	310	97	88	54	110	390	24	4	29	160
416–48–1, 84	42.75	15.93	10.47	3.40	1.23	3.42	0.75	n.d.	5.65	0.17	470	130	78	53	77	440	26	30	26	120
416–48–3, 9	52.35	18.29	2.91	3.11	1.20	4.11	0.77	n.d.	7.29	0.19	330	95	88	62	92	360	32	31	41	140
416–48–3, 85	50.50	19.94	2.24	3.19	1.18	3.58	0.75	n.d.	5.55	0.28	360	130	93	51	120	370	29	32	27	130
416–48–3, 101	53.40	19.71	2.38	2.34	1.11	3.43	0.70	n.d.	6.40	0.10	370	130	110	47	94	380	22	50	29	130
416–49–1, 6	48.30	14.87	9.77	2.32	1.16	2.59	0.71	n.d.	4.83	0.16	420	170	76	37	67	510	19	34	46	89
416–49–2, 33	43.60	9.32	17.71	2.20	0.84	2.47	0.54	n.d.	3.26	0.14	460	97	48	28	46	580	16	15	27	55
416–49–2, 40	54.40	18.20	2.00	3.34	1.53	4.11	0.83	n.d.	7.26	0.13	370	100	79	54	67	370	23	14	39	150
416–49–2, 109	40.45	14.75	13.48	2.74	1.08	3.10	0.60	n.d.	5.00	0.16	460	120	68	41	54	610	19	9	30	89
416–50–1, 1	51.25	18.11	2.63	3.19	1.58	3.95	0.73	n.d.	7.91	0.01	330	300	93	71	95	340	29	18	41	120
416–50–1, 14	21.95	7.14	31.68	1.95	0.61	1.58	0.25	n.d.	3.07	0.14	580	150	36	26	37	610	13	16	47	53
416–50–2, 2	48.45	11.39	13.76	1.99	0.86	2.26	0.54	n.d.	2.86	0.19	340	160	59	28	64	430	9	44	37	58
416–53–2, 3	15.75	5.43	35.00	2.28	1.11	1.39	0.18	n.d.	2.14	0.14	810	66	24	29	33	840	14	9	43	45
416–53–2, 13	52.35	17.47	4.59	3.05	1.20	4.14	0.77	n.d.	6.12	0.15	380	85	81	56	103	350	26	14	31	150
416–53–2, 32	60.10	13.92	3.40	3.15	1.77	3.77	0.64	n.d.	4.05	0.15	360	160	57	34	61	300	13	2	25	63
416–53–2, 142	50.00	18.23	3.78	3.48	1.25	3.95	0.72	n.d.	7.15	0.18	390	150	77	59	79	350	23	16	39	105
416–57–1, 23	50.80	19.29	2.28	3.56	1.21	4.14	0.73	n.d.	7.36	0.16	370	150	82	49	100	350	24	32	44	110
416–57–1, 99	53.45	18.39	2.66	3.37	1.18	4.28	0.79	n.d.	6.69	0.31	370	100	86	53	110	370	26	31	35	150

[a]Organic carbon.

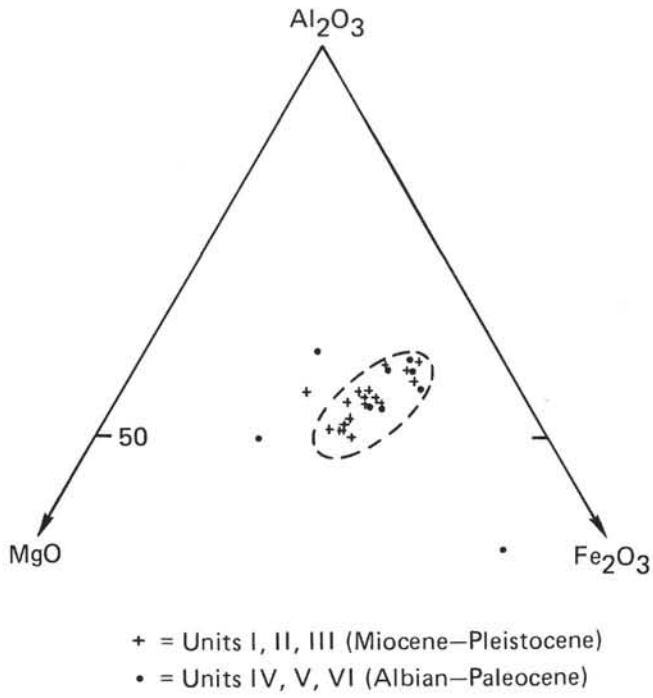

Figure 1. *Al_2O_3–F_2O_3–MgO diagram, Site 415.*

discussed below. It appears to involve enrichment in potassic minerals of the pre-Albian sediments of Site 416 (those minerals being distinctly marked by lithium).

A more distinct comparison between the two sites exists between the samples from the upper part of Hole 416 (Albian-Eocene). All variation domains of the chemical elements overlap (cf. K_2O and Li) and the concentrations of the major components (SiO_2, Al_2O_3, CaO, Fe_2O_3) are the same or very similar to each other. The identity of Al_2O_3 and Fe_2O_3 confirms a probable analogous clay source. Here the carbonate variations are essentially balanced by changes in the supply of detrital quartz. The similarity is equally obvious in the trace elements (cf. Mn, Zn, Ni, Cr, Sr, Co). Copper, however, at Site 415 and lead at the top of Site 416 are randomly distributed.

We can now confirm that the post-Albian sediments of Sites 415 and 416 are very similar, and that the pre-Albian deposits of Site 416 contain more aluminopotassic silicates (which confirms the clay-mineralogy studies of Chamley [this volume]). A greater supply of metalliferous trace elements (Ti, Mn, Li, Ni) was received at Site 416 than at Site 415.

Factor Analysis

A mathematical treatment characteristic of factor analysis in the *R* mode has been applied to the data from the two sites. The data from the two sites are considered separately in order to rapidly determine whether groups of elements (comparable or not) play a particular role in the whole set of geochemical variables.

TABLE 4
Geochemical Ratios, Site 416

Sample (interval in cm)	$\frac{SiO_2}{Al_2O_3}$	$\frac{Al_2O_3}{Fe_2O_3}$	$\frac{MgO}{K_2O}$	$\frac{Al_2O_3}{K_2O}$	$\frac{Na_2O}{K_2O}$	$\frac{Fe_2O_3}{K_2O}$	$\frac{Fe_2O_3}{MgO}$	$\frac{Sr\ 10^3}{CaO}$
416–1–1, 33	3.3	2.3	1.1	4.5	0.92	1.9	1.80	3.3
416–1–1, 44	3.4	2.3	1.1	3.2	0.72	1.4	1.3	3.4
416–1–1, 99	5.1	2.0	1.9	3.1	0.53	2.1	0.8	3.4
416–1–1, 117	3.9	2.2	1.3	3.8	0.67	1.7	1.4	3.4
416–1–2, 33	4.6	2.3	1.4	3.9	0.73	1.7	1.2	3.5
416–2–1, 31	4.4	2.2	1.4	3.5	0.47	1.6	1.2	3.3
416–2–3, 64	4.8	2.2	1.2	3.4	0.56	1.6	1.4	3.4
416–3–3, 39	4.0	2.6	1.0	3.8	0.43	1.5	1.5	2.1
416–3–3, 47	4.5	2.1	1.3	3.3	0.45	1.4	1.2	3.5
416–6–3, 3	4.6	2.9	0.5	4.0	0.40	1.7	2.7	114.3
416–7–2, 122	3.3	3.2	0.6	4.7	0.35	1.5	2.40	11.4
416–9–2, 12	3.9	2.4	0.7	4.5	0.42	1.9	2.6	4.0
416–10–1, 61	2.6	2.4	0.7	4.9	0.34	2.0	3.1	13.8
416–11–3, 4	2.3	3.5	0.8	6.1	0.35	1.7	2.1	8.8
416–11–3, 9	3.8	3.2	0.8	5.6	0.58	1.8	2.3	15.7
416–12–1, 108	3.9	1.7	1.1	4.3	0.54	2.5	2.3	2.9
416–12–1, 147	2.6	2.9	0.7	5.0	0.33	1.7	2.6	17.3
416–13–2, 67	2.3	2.6	0.7	5.2	0.30	2.0	2.9	5.8
416–14–1, 105	2.6	2.4	0.8	5.0	0.31	2.1	2.7	5.7
416–16–1, 25	2.4	3.1	0.7	5.0	0.28	1.6	2.4	7.3
416–18–1, 137	3.1	2.2	0.8	4.4	0.36	2.0	2.6	3.3
416–19–2, 82	2.6	2.8	0.7	4.4	0.29	1.6	2.3	69.6
416–19–2, 101	3.4	1.4	1.1	4.0	0.45	2.9	2.7	2.7
416–20–1, 99	2.8	2.6	0.8	5.1	0.38	2.0	2.4	5.8
416–21–1, 10	3.4	1.9	1.2	4.4	0.45	2.4	2.0	2.6
416–23–2, 16	2.8	2.0	0.9	4.8	0.42	2.4	2.6	3.0
416–25–1, 97	2.7	2.5	0.8	5.0	0.37	2.0	2.6	17.2
416–25–1, 140	2.9	2.7	1.2	1.3	0.4	2.0	1.7	2.7
416–25–1, 147	2.3	2.4	0.8	5.4	0.31	2.0	2.6	13.2
416–29–3, 23	3.4	1.8	1.3	4.8	0.44	2.2	2.0	2.6
416–33–5, 60	3.0	2.5	0.8	4.6	0.37	2.7	2.3	7.2
416–36–1, 16	4.1	2.4	0.9	5.0	0.5	1.8	2.3	5.4
416–36–1, 129	2.3	2.7	0.9	6.1	0.32	2.1	2.5	5.0
416–36–2, 8	4.8	2.5	0.9	5.0	0.62	2.0	2.1	4.6
416–36–3, 28	2.6	3.3	1.0	6.4	0.38	2.0	2.0	13.3
416–37–2, 77	3.1	2.6	0.7	4.7	0.31	1.8	2.5	12.3
416–37–3, 10	4.6	1.4	2.0	4.2	0.41	2.9	1.4	2.6
416–37–4, 7	2.2	3.2	0.8	6.6	0.28	2.1	2.5	9.1
416–38–1, 11	3.1	3.0	0.8	5.1	0.39	1.7	2.1	4.1
416–38–1, 44	3.7	2.1	0.8	3.7	0.30	1.8	2.3	8.8
416–38–2, 18	2.3	2.6	0.8	5.1	0.27	2.0	2.4	3.0
416–40–6, 4	4.0	2.4	0.8	3.8	0.36	1.6	2.0	12.1
416–40–6, 17	2.3	3.5	0.9	5.9	0.30	1.7	1.9	3.4
416–40–6, 22	2.6	2.8	0.9	5.4	0.34	2.0	2.2	11.9
416–42–2, 125	2.1	3.1	0.8	6.2	0.29	2.0	2.6	1.3
416–43–1, 46	3.0	2.2	0.7	4.6	0.28	2.9	2.9	9.4
416–43–2, 51	3.4	2.9	1.0	5.6	0.5	2.0	1.9	4.2
416–43–4, 56	2.4	2.7	0.8	5.3	0.30	2.0	2.4	8.9
416–43–4, 80	2.6	2.8	1.0	5.2	0.43	1.9	1.8	18.0
416–44–1, 11	3.4	2.7	0.8	4.6	0.42	1.7	2.2	4.2
416–44–2, 1	2.5	3.7	0.8	5.4	0.33	1.5	1.8	26.2
416–44–2, 7	3.0	3.0	0.8	4.4	0.30	1.5	2.0	21.1
416–44, CC, 12	2.4	2.5	1.11	4.6	0.29	1.9	1.6	1.6
416–46–2, 8	3.7	3.8	0.8	5.3	0.51	1.4	1.7	8.8
416–46–2, 10	3.3	3.2	0.8	4.8	0.39	1.5	2.0	9.4
416–46–4, 100	2.8	2.3	0.9	4.8	0.29	2.1	2.3	8.3
416–46–4, 104	4.0	4.0	0.8	5.1	0.54	1.3	1.5	10.4
416–46–4, 110	2.8	3.5	0.8	4.9	0.32	1.4	1.7	18.0
416–48–1, 84	2.7	2.8	1.0	4.7	0.36	1.7	1.7	4.2
416–48–3, 9	2.9	2.5	0.8	4.4	0.29	1.8	2.3	12.4
416–48–3, 85	2.5	3.6	0.9	5.6	0.33	1.6	1.7	16.5
416–48–3, 101	2.7	3.1	0.7	5.8	0.32	1.3	2.7	16.0
416–49–1, 6	3.2	3.1	0.9	5.7	0.45	1.9	2.1	5.2
416–49–2, 33	4.7	2.9	0.9	3.8	0.34	1.3	1.5	3.3
416–49–2, 40	3.0	2.5	0.8	4.4	0.37	1.8	2.2	18.5
416–49–2, 109	2.7	3.0	0.9	4.8	0.35	1.6	1.8	4.5
416–50–1, 1	2.8	2.3	0.8	4.6	0.4	2.0	2.5	12.9
416–50–1, 14	3.1	2.3	1.2	4.5	0.39	1.9	1.6	1.9
416–50–2, 2	4.3	4.0	0.9	5.0	0.38	1.3	1.4	3.1
416–53–2, 3	2.9	2.5	1.6	3.9	0.80	1.5	0.9	2.4
416–53–2, 13	3.0	2.9	0.7	4.2	0.29	1.5	2.0	7.6
416–53–2, 32	4.3	3.4	1.1	5.0	0.64	1.5	1.3	8.8
416–53–2, 142	2.7	2.6	0.9	4.6	0.32	1.8	2.1	9.3
416–57–1, 23	2.6	2.6	0.9	4.7	0.29	1.8	2.1	15.4
416–57–1, 99	2.9	2.8	0.8	4.3	0.28	1.6	2.0	13.9

We have limited our study to the search for factors on orthogonal axes using an iterative method on the correlations matrix (factor analysis in principal components). The calculation was carried out for five factors.

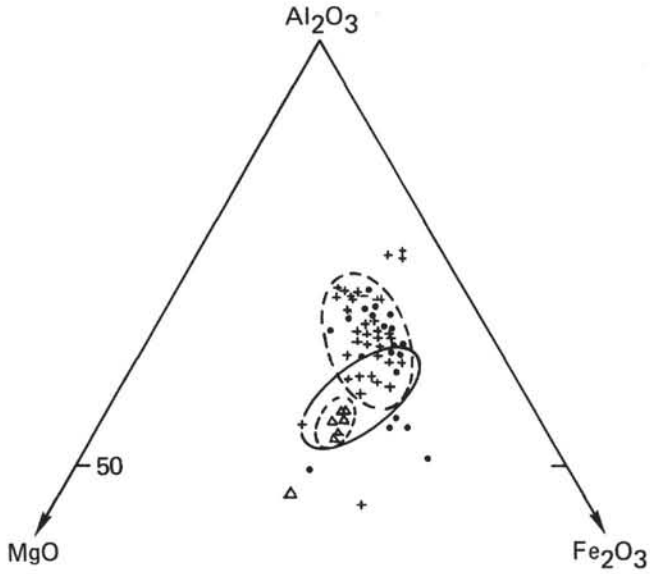

△ = Units I, II (Eocene–Pleistocene)
• = Unit VI (Valanginian–Barremian)
+ = Unit VII (Tithonian–Valanginian)
——— = Site 415 data

Figure 2. *Al_2O_3–Fe_2O_3–MgO diagram, Site 416.*

TABLE 5
Mean Chemical Compositions, Leg 50 Sites

	Site 415		Site 416 (all samples)		Site 416 (Albian–Pleistocene)	
	$\bar{X}$	σ	$\bar{X}$	σ	$\bar{X}$	σ
SiO_2 (%)	30.9	14.2	45.3	11.4	35.2	11.7
Al_2O_3	8.2	4.1	14.9	4.8	8.3	2.6
CaO	24.6	12.4	10.5	10	20.5	10.6
MgO	2.2	0.8	2.7	0.6	3.0	1.0
Na_2O	1.3	0.4	1.2	0.3	1.3	0.2
K_2O	1.3	0.5	3.1	0.8	2.3	0.7
TiO_2	0.44	0.23	0.62	0.20	0.35	0.18
Fe_2O_3	3.6	1.8	5.6	1.5	3.7	1.0
Mn (ppm)	320	170	420	150	340	40
Zn	75	27	113	40	84	18
Li	35	9	64	24	53	16
Ni	34	9	51	25	29	7
Cr	76	45	102	47	73	31
Sr	850	380	470	190	700	350
Co	13	4	20	7	10	4
Cu	31	56	25	17	27	13
Pb	24	17	41	38	72	100
V	100	47	113	35	79	31

Note: $\bar{X}$ = mean concentration; σ = root mean square deviation.

Site 415 (Figure 3)

Owing to the small number of samples and to the lack of dispersion of the data, five factors account for nearly 89 per cent of the global variance.

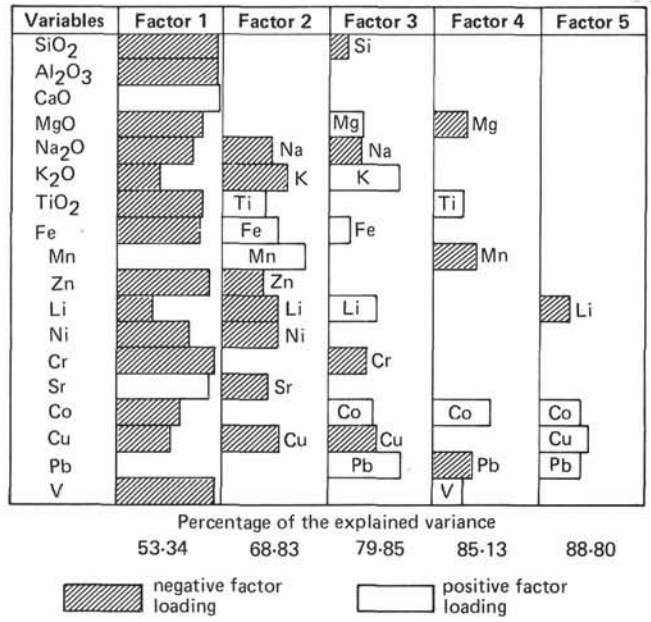

Figure 3. R *mode factor analysis, Site 415 analyses.*

Except for K_2O among the major elements, and Mn, Li, and Pb among the trace elements, all the variables occur heavily weighted in the first factor, which represents 53 per cent of the global variance. This factor can be defined as the negative correlation between the strontian carbonate phase and the aluminosilicate phases. The relationship is made evident by the signs affecting each variable.

If we arrange the variables of the first factor in order of weights for the major elements (Al_2O_3, SiO_2, MgO, Fe, Na_2O, . . .) and then for the trace elements (Cr, V, Zn, Ti, Ni, . . .), we see in the silicates the dominant ferromagnesian character of the smectite-fibrous clay mixture defining the clay base of most of the samples (at least below the Miocene). Furthermore, we note that most of the trace elements are preferentially tied to the clay minerals (Cr, V, Zn, Ti, Ni, Co), whereas Mn and Pb seem to be independent.

The second factor is marked by a negative correlation between the groups Mn-Fe on one hand and K_2O, Li, Ni, Cu on the other. Most of these elements are poorly represented in the first factor. We interpret this as an opposition between the supply of potassic clay minerals marked by lithium and nickel, and metalliferous precipitations in an oxidizing environment (Fe, Mn). This second factor might be characteristic of the post-Eocène period because we detected illitic contributions from the Miocene upwards. Moreover, the occurrence of most manganese is related with carbonate to the top of that series, whereas the iron and manganese most frequently co-exist in the oxide form. (Goethite is reported by Chamley [this volume] in Sample 415B-2-1, 44 cm.)

The third factor is defined only by a potassic phase apparently marked by lithium, lead, and cobalt. Cobalt occurs ubiquitously and seems to be distributed among the alumino-ferrous and potassic silicates.

Factors 4 and 5 are not very explicit because each are defined by one single element of sufficent weight: cobalt (factor 4) and copper (factor 5). Each element behaves a particular way.

Site 416 (Figure 4)

Five factors explain only 78 per cent of the global variance, which confirms the heterogeneity of the samples collected at that site.

As for Site 415, the first factor is characterized by the negative correlation between the silicate and carbonate phases, but the composition of those phases is distinct at the two sites. In arranging the variables of the first factor in order of decreasing weights of the same sign, we obtain K_2O, Al_2O_3, SiO_2, Fe, MgO, Na_2O, . . . for the major elements and Ti, V, Co, Cr, Ni, Li, . . . for the trace elements. The dominant clay base is thus clearly alumino-potassic and ferruginous instead of magnesian, whereas lithium and manganese play a large role in the general covariance. The carbonate phase is marked by strontium and to a lesser degree by manganese. The presence of manganese at that level is a second difference from the Site 415 sequence.

The second factor, defined by trace elements, shows the negative correlation between the (Ni, Cr, Pb) group and lithium; those elements mark different clay-mineral phases. The presence of lead, however, is difficult to explain inasmuch as lead is practically independent at the level of the first factor.

The third factor is marked by a negative correlation between sodium and the vanadium–manganese couple, but the interpretation of that correlation is still unexplained.

In the fourth factor, the lead-strontium linkage results because part of the lead is tied to the carbonates.

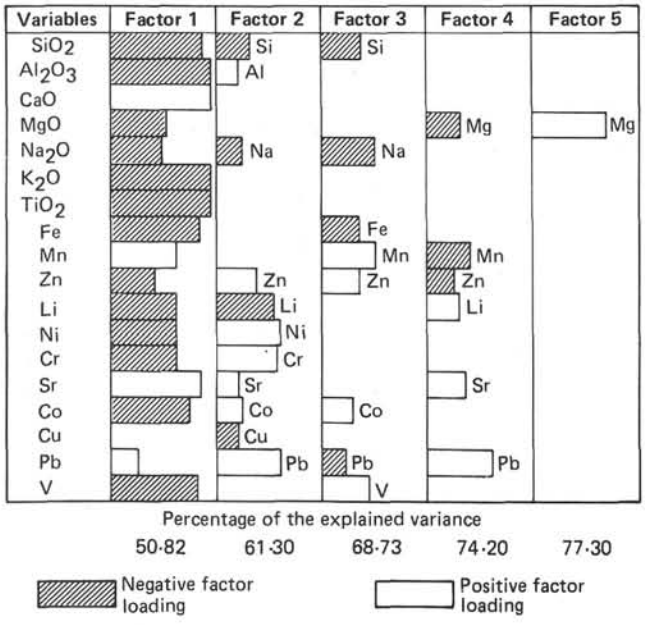

Figure 4. R *mode factor analysis, Site 416 analyses.*

This relationship could account for the sign observed for lead in the first factor.

Lastly, the fifth factor is, as at Site 415, defined by the fluctuation of copper, which is a particularly independent element in the various sites that have been studied.

Total Correlations

In this study, we deal with properties being either characteristic of each site or common to both of them. Only the correlation coefficients that were significant at a probability threshold of 0.01 (Fisher test) have been retained; the range of variation is too great from 0.02 onward. Most of the relationships elicited above are also found in this aspect of the study.

Site 415 (Table 6)

The major silicate phase is defined by the grouping of highly covariant oxides Al_2O_3 (SiO_2, Fe_2O_3, MgO) reflecting the clear dominance of ferro-magnesian silicates (smectite) which constitute the larger part of the clay mineral assemblage of the pre-Miocene samples.

A close examination of the demonstrated interrelationships reveals the existence of a sodic silicate phase marked by zinc, and one that contains the small amounts of copper seen in the core: SiO_2 (Na_2O, Zn, Cu). The particular covariance of Na_2O and its intense linkage with silica were previously found in fibrous-clay levels at Site 398 (Debrabant et al., unpublished manuscript).

An apparently independent potassic phase indicates completely different origins for illite and smectite, which is confirmed by metalliferous markers. Lithium marks the potassic phase only, whereas titanium, chromium, and vanadium mark the ferromagnesian phase. Nickel is ubiquitous; cobalt, weakly covariant, tends to mark alumino-ferrous levels.

Chromium and silica (R^1 = 0.97) are particularly strongly related and also occur in the post-Albian sediments of Site 416 (Figure 5).

Also the Al_2O_3-TiO_2 couple from Miocene sediments upward form an almost linear relationship; the data are more scattered in older sediments. Finally, manganese and lead seem to be totally independent. In the pre-Miocene sediments (Figure 6) manganese is mainly bound to calcium carbonates, but in Miocene sediments and upward it seems to occur only in the oxidized state. This could result from diagenesis caused by a more intense degree of oxidation in the shallower sediments.

Lastly, the CaO-Sr association is in opposition to the silicate phase. However, the association of the two elements of this classical couple seems to be discontinuous (Figure 7). The data points seem to align along two separate straight lines, and show a break somewhere between the Paleocene and Miocene samples. For identical amounts of lime, strontium concentrations in-

[1] R = correlation coefficient.

TABLE 6
Probable Correlations (limit 0.01 – Fisher's Test), Site 415

	SiO_2	Al_2O_3	CaO	MgO	Na_2O	K_2O	TiO_2	Fe_2O_3	Mn	Zn	Li	Ni	Cr	Sr	Co	Cu	Pb
Al_2O_3	0.87																
CaO	−0.98	−0.94															
MgO	0.73	0.80	−0.80														
Na_2O	0.70	0.58	−0.67														
K_2O																	
TiO_2	0.73	0.94	−0.82	0.65													
Fe_2O_3	0.68	0.85	−0.73	0.66			0.87										
Mn																	
Zn	0.88	0.74	−0.84		0.81												
Li						0.78											
Ni	0.64		−0.63	0.61	0.76	0.60				0.75							
Cr	0.97	0.81	−0.94	0.67	0.74		0.64	0.61		0.85		0.63					
Sr	−0.87	−0.85	0.89	−0.69			−0.81	−0.86		−0.66			−0.82				
Co		0.62					0.58	0.63									
Cu	0.55				0.71					0.73			0.66				
Pb																	
V	0.82	0.93	−0.87	0.65	0.61		0.86	0.82		0.71			0.79	−0.89	0.60		

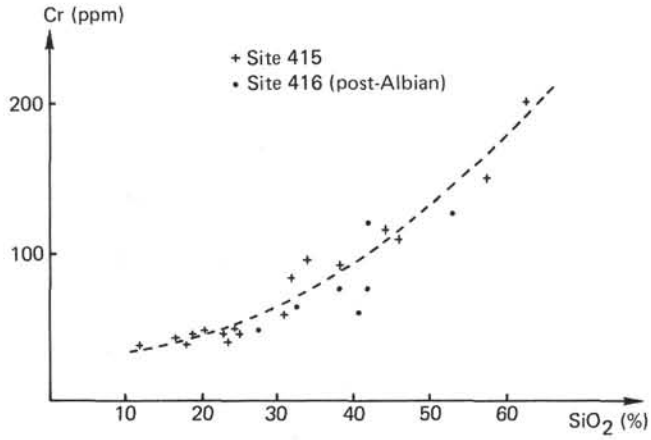

Figure 5. *Variation of Cr content as a function of SiO_2 content, Sites 415 and 416.*

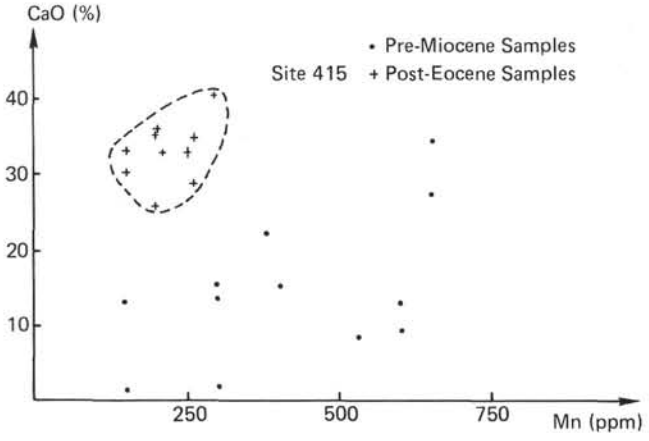

Figure 6. *Variation of CaO content as a function of Mn content, Site 415.*

crease markedly from the Miocene sediments upwards. Here again the carbonate could be of diagenetic origin or it could reflect the more pelagic character of the environment.

Site 416 (Table 7)

The study of total correlations for this site shows that the most covariant set is an alumino-potassic and ferriferous phase Al_2O_3 (K_2O, Fe_2O_3, TiO_2). Magnesium seems to intervene to a much lesser degree in the whole core. However, the relationships within the trace elements are much the same as at Site 415.

Though it plays a large part in the general covariance, lithium shows its closest linkage with the potassic phase (represented throughout the sampling). Titanium is closely bound to the whole set of alumino-ferriferous and potassic clay minerals. However, its linkage with aluminum is not a simple one. TiO_2 increases regularly together with aluminum up to the level of 14 per cent of Al_2O_3. Beyond that percentage, the TiO_2 content becomes stable between 0.65 per cent and 0.85 per cent (Figure 8). This phenomenon cannot be explained easily, because extra quantities of aluminum can originate from a clay mineral not readily susceptible to titanium replacements.

Nickel, chromium, and cobalt seem to be ubiquitous, whereas vanadium behaves like titanium. Last, copper and lead rank in secondary position, whereas copper is totally independent.

The carbonate phase, marked not only by strontium but also by manganese is, of course, in opposition to the silicate phase. This relation is far from being a persistent one (Figure 9); it disappears from the Eocene and above. Strontium behaves very much the same way (Figure 7). The graphic representation of Sr versus CaO produces, as for Site 415, two separate straight lines when pre- and post-Paleocene samples are separated.

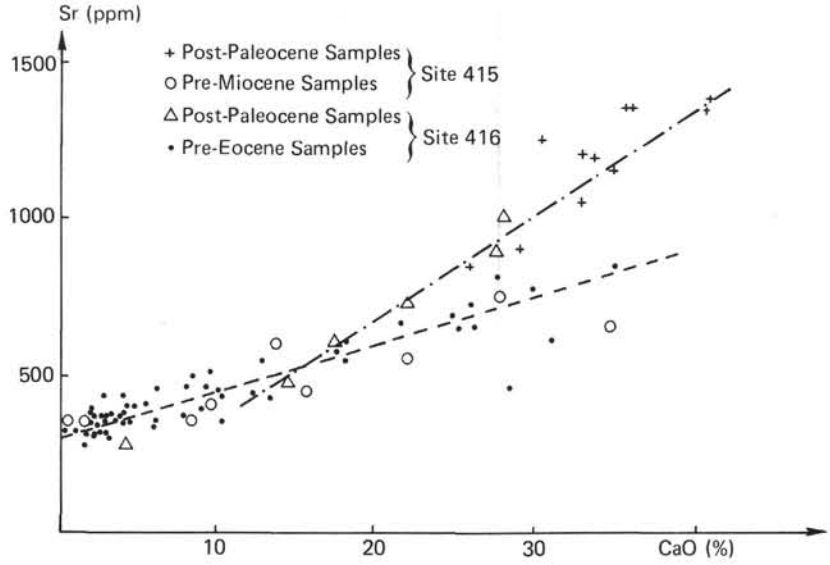

Figure 7. *Variation of Sr content as a function of CaO content, Sites 415 and 416.*

CONCLUSIONS

We cannot easily compare the two sites (415 and 416) of Leg 50 because of the stratigraphic difference of the two series concerned. For example, the ferro-potassic character of Site 416 is largely contributed by pre-Albian sediments which are absent from Site 415. Site 415 has a marked ferromagnesian character. Certain criteria, however, which may indicate that Site 415 material is more characteristic of a more-oceanic environment than that of Site 416, are worth noting. Furthermore, an environmental change which seems to correspond to more open sea conditions occurred simultaneously at both sites after the Paleocene. Our data are also comparable with the results obtained at the more northerly sites (398 and 400). At those sites, the major alumino-ferriferous phase is marked by the same grouping of trace elements (Ti, V, Cr), whereas lithium tends to characterize the more potassic minerals (which was previously noted in Leg 47B).

Fibrous clay minerals (Site 415) are accompanied (as at Site 398) by a stronger covariance of sodium and magnesium. Below the Tertiary sediments the carbonate phase, which is inversely related to the silicate phase, is marked not only by strontium but also by manganese. This tendency was also noted in Site 398 samples.

Metalliferous precipitations occur in Albian to Eocene sediments from the deeper site of the Bay of Biscay. The stratigraphic limits of that phenomenon corresponded with intervals rich in fibrous clay minerals and

TABLE 7
Probable Correlations (limit 0.01 – Fisher's Test), Site 416

	SiO_2	Al_2O_3	CaO	MgO	Na_2O	K_2O	TiO_2	Fe_2O_3	Mn	Zn	Li	Ni	Cr	Sr	Co	Cu	Pb
Al_2O_3	0.72																
CaO	−0.95	−0.87															
MgO	0.37	0.40	−0.48														
Na_2O	0.64	0.30	−0.57	0.34													
K_2O	0.79	0.88	−0.91	0.56	0.45												
TiO_2	0.85	0.87	−0.92	0.33	0.45	0.88											
Fe_2O_3	0.55	0.83	−0.74	0.43		0.82	0.74										
Mn	−0.68	−0.51	0.65	−0.31	−0.59	−0.60	−0.57										
Zn		0.46	−0.35	0.30		0.32		0.33									
Li	0.51	0.50	−0.61			0.66	0.62	0.55	−0.35								
Ni	0.35	0.69	−0.50	0.34		0.54	0.50	0.62		0.51							
Cr	0.44	0.73	−0.56	0.33		0.53	0.51	0.56	−0.41	0.48		0.78					
Sr	−0.88	−0.74	0.89	−0.50	−0.44	−0.78	−0.79	−0.63	0.47	−0.40	−0.45	−0.42	−0.52				
Co	0.44	0.74	−0.61	0.34		0.73	0.70	0.71	−0.32	0.34	0.49	0.68	−0.44	−0.46			
Cu																	
Pb	−0.34		0.32								−0.39			0.52			
V	0.55	0.78	−0.71	0.31		0.79	0.79	0.79	−0.35		0.72	0.47	0.46	−0.57	0.73		

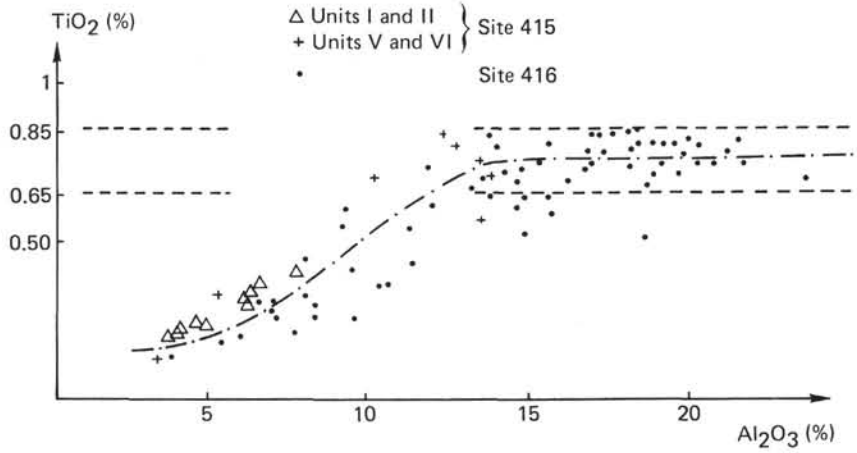

Figure 8. *Variation of TiO_2 content as a function of Al_2O_3 content, Sites 415 and 416.*

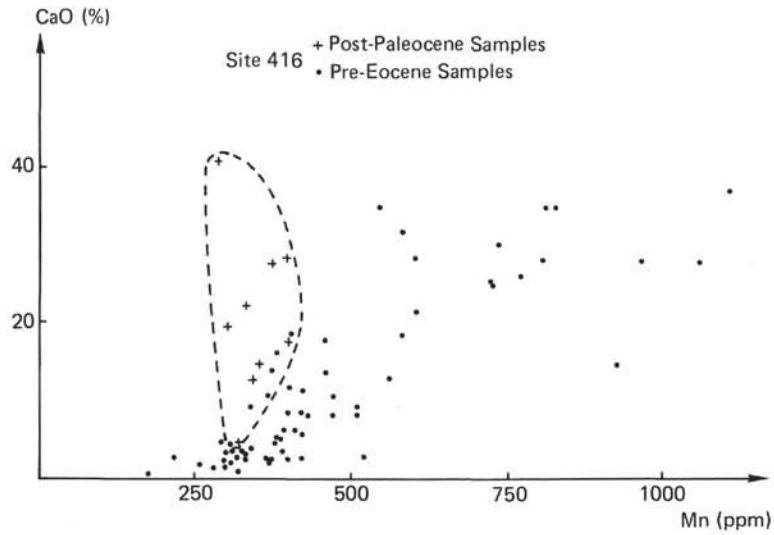

Figure 9. *Variation of CaO content as a function of Mn content, Site 416.*

may have been caused by deep currents. Nothing similar was noted in the Leg 50 material, not even that from Site 415 which is rich in attapulgite. We thus formulate two hypotheses. Depths at Leg 50 sites were either approximately the same as at Site 402 (Leg 48), or the metalliferous carrier originated from the north and encountered the fibrous-clay carrier in the area of the Bay of Biscay, thus favoring the precipitation of transition elements.

ACKNOWLEDGMENTS

We are grateful to the U. S. National Science Foundation and to the shipboard team of Leg 50 for allowing us to conduct the investigations. We received financial support for the study from CNRS (France) through Grants ATP-IPOD. The geochemical study of carbon was realized thanks to the technical assistance of R. Jouglet and the mathematical treatment was worked by M. Meunier. We gratefully acknowledge W. R. Riedel and R. Létolle for reviewing the manuscript.

REFERENCES

Chamley, H., Debrabant, P., Foulon, J., Giroud D'Argoud, G., Latouche, C., Maillet, N., Maillot, H., and Sommer, F., 1979. Mineralogy and geochemistry of Cretaceous and Cenozoic Atlantic sediments of the Iberian peninsula (Site 398, DSDP Leg 47B). *In* Ryan W., Sibuet, J.-C., et al., *Initial Reports of the Deep Sea Drilling Project,* v. 47, Part 2: Washington (U.S. Government Printing Office).

Debrabant, P., Chamley, H., Foulon, J., and Maillot, H., 1979. Mineralogy and geochemistry of Upper Cretaceous and Cenozoic sediments from North Biscay Bay and Rockall Plateau (Eastern North Atlantic), DSDP Leg 48. *In* Montadert, L., Roberts, D.G., et al., *Initial Reports of the Deep Sea Drilling Project,* v. 48: Washington (U.S. Government Printing Office), p. 703–726.

Deer, W.A., Howie, R.A., and Zussman, J., 1963. *Rock forming minerals, Sheet silicates:* (Longmans), v.3.